Q_y-Excitation Resonance Raman Spectra of Chlorophyll *a* and Related Complexes. Normal Mode Characteristics of the Low-Frequency Vibrations

Chengli Zhou, James R. Diers, and David F. Bocian*

Department of Chemistry, University of California, Riverside, California 92521-0403

Received: June 16, 1997; In Final Form: September 11, 1997[⊗]

Q_y-excitation resonance Raman (RR) spectra are reported for film aggregates of chlorophyll (Chl) *a* and a series of related complexes. The latter include Mg(II) octaethylporphyrin (MgOEP), Mg(II) *trans*-octaethylchlorin (MgOEC), methyl-9-desoxomesopyrochlorophyllide (DMPChl) *a*, and methylpyrochlorophyllide (MPChl) *a*. These complexes represent a series in which the structural complexities of Chl *a* (saturated pyrrole ring, isocyclic ring, C_9-keto group, C_2-vinyl group, and C_{10}-carbomethoxy group) are systematically added to the basic tetrapyrrole architecture. On the basis of comparison of the RR scattering characteristics of the different complexes and the predictions of semiempirical normal coordinate calculations, a self-consistent set of vibrational assignments has been developed for all the RR active modes in the low-frequency regime (100−1000 cm^{-1}). The studies indicate that the low-frequency vibrations encompass a diverse set of motions that include both the ring skeleton and peripheral substituent groups. However, modes in the very low-frequency regime (<250 cm^{-1}) are primarily due to deformations of the substituent groups. Collectively, the normal mode characteristics of Chl *a* and the other Mg(II) complexes provide insights into the nature of the vibrational modes that are coupled to the photophysically important, lowest energy excited states of natural photosynthetic assemblies.

Introduction

Chlorophylls and bacteriochlorophylls serve as the photophysically active pigments in the photosynthetic assemblies of plants and bacteria.[1] The (bacterio)chlorophylls differ from porphyrins in that one or two of the pyrrole rings are saturated (hydroporphyrins) and a fifth, isocyclic ring is added to the basic tetrapyrrole architecture. The structural differences in (bacterio)-chlorophylls versus porphyrins lead to altered photophysical and redox properties between the different classes of macrocycles.[2] The altered nature of these physical properties is presumably responsible for the evolutionary selection of hydroporphyrins as the active pigments in photosynthetic systems.

Resonance Raman (RR) spectroscopy provides a convenient and direct method for probing both the ground- and excited-state properties of chromophores via the characteristics of the RR frequencies and intensities, respectively.[3] To date, RR spectroscopic methods have been used to investigate a variety of photosynthetic pigments, both in isolated form and in protein systems.[4] The majority of these studies have focused on the high-frequency (1000−1750 cm^{-1}) region of the spectrum which contains bands due to ring-skeletal and carbonyl stretching vibrations of the macrocycle.[4−6] These vibrational data have been used to assess the conformation of the (bacterio)chlorophyll rings, the ligation state of the Mg(II) ion, and the extent of hydrogen bonding to the carbonyl substituents on the rings. Despite the focus on high-frequency vibrations, the low-frequency (<1000 cm^{-1}) region of the spectrum, which contains bands primarily due to ring-skeletal and substituent deformations,[4] is of considerable interest. For example, it has been shown that low-frequency vibrational modes are strongly coupled to the electronic transition which initiates the primary charge-separation process in reaction center proteins[7−14] and the transitions that mediate the energy-transfer process in light-harvesting assemblies.[15,16] The exact identity of the low-frequency vibrational modes involved in these processes has only recently begun to be elucidated.[13c−e,17]

Both the charge-separation and energy-transfer processes in photosynthetic assemblies are mediated by the lowest energy, Q_y-excited states of the cofactors.[2a,c] Accordingly, RR probes of the photophysically relevant vibronically coupled modes must utilize Q_y-excitation. In the case of certain natural photosynthetic assembles, such as reaction centers and chlorosomes, the acquisition of Q_y-excitation RR spectra is possible because the high level of fluorescence intrinsic to free (bacterio)chlorophylls is strongly quenched in the pigment−protein complexes by ultrafast energy- and/or electron-transfer processes.[13,14] Recently, our group has found that Q_y-excitation RR spectra can also be obtained for free (bacterio)chlorophylls in a solid film environment.[17] The film environment red shifts and/or significantly quenches the emission from the pigments. The opportunity to obtain Q_y-excitation RR spectra of photosynthetic pigments external to pigment−protein complexes is essential for establishing a complete set of benchmarks for characterizing the vibronically coupled modes.

In this paper, we report low-frequency Q_y-excitation RR spectra of film aggregates of chlorophyll (Chl) *a* and a series of related complexes. The structures of the complexes investigated are shown in Figure 1 and include Mg(II) octaethylporphyrin (MgOEP), Mg(II) *trans*-octaethylchlorin (MgOEC), methyl-9-desoxomesopyrochlorophyllide (DMPChl) *a*, and methylpyrochlorophyllide (MPChl) *a*, in addition to Chl *a*. These complexes represent a series in which the structural complexities of Chl *a* (saturated pyrrole ring, isocyclic ring, C_9-keto group, C_2-vinyl group, and C_{10}-carbomethoxy group) are systematically added to the basic tetrapyrrole architecture. The focus of the studies is on the low-frequency vibrational modes of the complexes. The present studies build on earlier work from our laboratory which elucidated the high-frequency, Q_y-excitation RR scattering characteristics of this same series of complexes.[18] [The earlier studies were performed on Ni(II) complexes rather than on Mg(II) species because it was not known at the time

[⊗] Abstract published in *Advance ACS Abstracts,* November 1, 1997.

S1089-5647(97)01965-2 CCC: $14.00

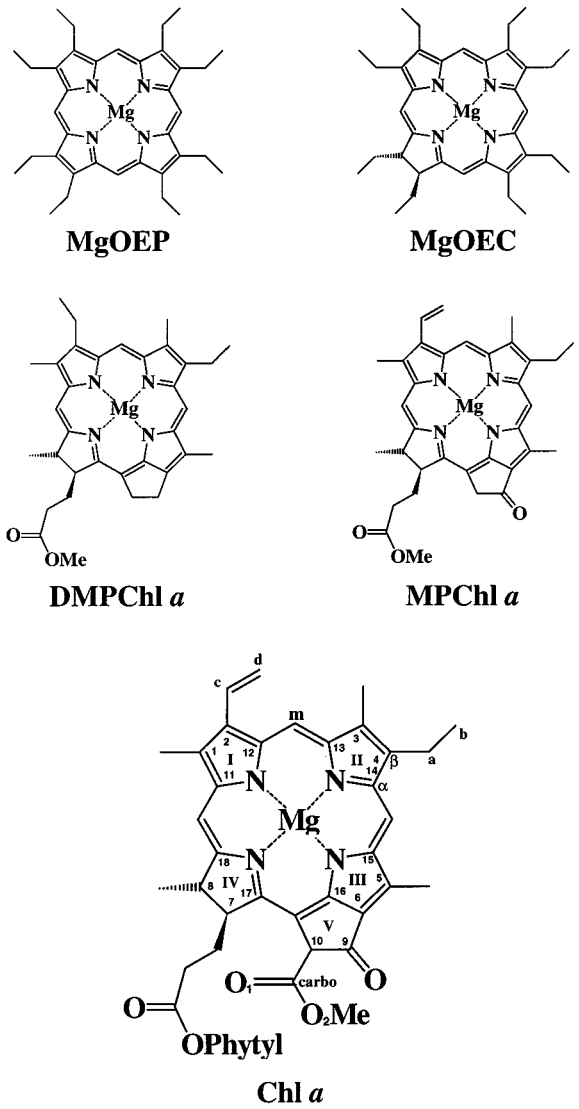

Figure 1. Structures and labeling scheme for the Mg(II) complexes.

that fluorescence from the Mg(II) complexes is sufficiently quenched in film aggregates to permit acquisition of Q_y-excitation RR spectra.[17] Consequently, fluorescence quenching was achieved via replacement of the closed shell Mg(II) ion with the open shell Ni(II) ion.[18]] In addition to the RR spectroscopic studies reported herein, normal mode descriptions are obtained for the low-frequency modes using the QCFF/PI method of Warshel and Karplus.[19] Together, the RR studies and the normal coordinate calculations provide a more detailed assessment of the nature of the vibrational modes which are coupled to the Q_y-transitions in Chl *a* type pigments.

The organization of the paper is as follows. First, we present the results of the RR study and summarize the assignments for the low-frequency vibrational modes. Next, we discuss the strategy for obtaining the vibrational assignments. We then discuss the influence of the different structural elements (saturated pyrrole ring, isocyclic ring, C_9-keto group, C_2-vinyl group, and C_{10}-carbomethoxy group) on the RR spectral features and normal mode descriptions. Finally, we comment on the implications of the present work for understanding the nature of the vibrational modes that are coupled to the Q_y-state transitions of pigments in natural photosynthetic assemblies.

Experimental Section

Sample Preparation. MgOEP was prepared from OEP (Midcentury Chemicals, Posen, IL) by the method of Lindsey et al.[20] using $MgBr_2$ (etherate) (Aldrich) as the metal source and triethylamine as the base. The product was purified on an alumina column with CH_2Cl_2 elution yielding residual OEP and with CH_2Cl_2/acetone (1:1) elution affording MgOEP. *trans*-OEC was obtained from OEP by the method of Whitlock et al.[21] Magnesium was inserted by the method of Lindsey et al.[20] MgOEC was purified in the same manner as described for MgOEP. Chl *a* was isolated from spray-dried *Spirulina maxima* algae (Earthrise Co., San Rafael, CA) according to the method of Smith et al.[22] The crude product was dissolved in a minimal amount of CH_2Cl_2 and chromatographed on an alumina column. The elution was initiated with *n*-hexane and then followed by CH_2Cl_2 to remove the neutral products. Chl *a* was the major green band collected by using 0.5−5% (v/v) propanol in CH_2Cl_2 as the eluting solvent. MPChl *a* was prepared from methyl pyropheophorbide *a* which was obtained from Chl *a* by the method of Smith et al.[22] Magnesium was inserted by the method of Lindsey et al.[20] MPChl *a* was purified on a sugar column using *n*-hexane as the eluting solvent. MDPChl *a* was prepared from methyl-9-desoxomesopyropheophorbide *a* by the method of Abraham et al.,[23] in which magnesium was inserted by using ethylmagnesium bromide and 2,6-di-*tert*-butyl-4-methylphenol. Methyl-9-desoxomesopyropheophorbide *a* was obtained from methylmesopyropheophorbide *a* using $NaBH_4$ and trifluoroacetic acid. This compound was chromatographed on a flash silica gel column eluting with 1% MeOH−99% CH_2Cl_2. Methyl-mesopyropheophorbide *a* was prepared by the method of Smith et al.[22]

RR Spectroscopy. Q_y-excitation RR spectra were recorded at low temperature (15 K) on films deposited directly onto the cold tip of a closed cycle He refrigeration system (ADP Cryogenics, DE 202 Displex). The procedure for preparing the films has been described in detail previously.[17] B-excitation RR spectra were collected for both film (15 K) and solution (293 K) samples of selected complexes. For the solution studies, benzene and CCl_4 were used as the solvents to obtain data in the spectral window below and above 900 cm^{-1}, respectively. The RR scattering was collected at 90° to the incident laser beam by using a camera lens (Canon 50 mm *f*/1.4) and dispersed by a triple spectrograph (Spex 1877) equipped with either a 1200 groove/mm (Q_y-excitation) or 2400 groove/mm (B-excitation) grating in the final stage. The detection system was a 1152 × 298 pixel, front-illuminated, UV-enhanced charge-coupled device (Princeton Instruments LN/CCD equipped with a EEV 1152-UV chip). The excitation wavelengths were provided by the outputs of a Kr ion laser (Coherent Innova 200-K3) or a dye laser (Coherent CR-590) using Rhodamine 590 (Exciton Chemical Co.) pumped by the multiline visible output of an Ar ion laser (Coherent Innova 400-15UV). The laser powers at the sample were typically 2 mW. The frequencies were calibrated using the known frequencies of indene or CCl_4.

Normal Coordinate Calculations. The vibrational frequencies and eigenvectors for the low-frequency modes of the Mg(II) complexes were obtained using the QCFF/PI method.[19] The calculations were performed as described in our earlier studies of the Ni(II) analogues of the complexes.[18] However, in the present analysis, the methyl, ethyl, and vinyl substituent groups were explicitly included in the calculations rather than being treated as point masses. The keto fragment of the carbomethoxy group and the ring-adjacent methylene group of the propionate ester were also explicitly included in the calculations. The methoxy fragment of the former substituent and the remainder of the latter substituent were treated as 15 amu point masses. The torsional coordinates of all the substituent groups were unconstrained in the energy minimizations. In the resulting

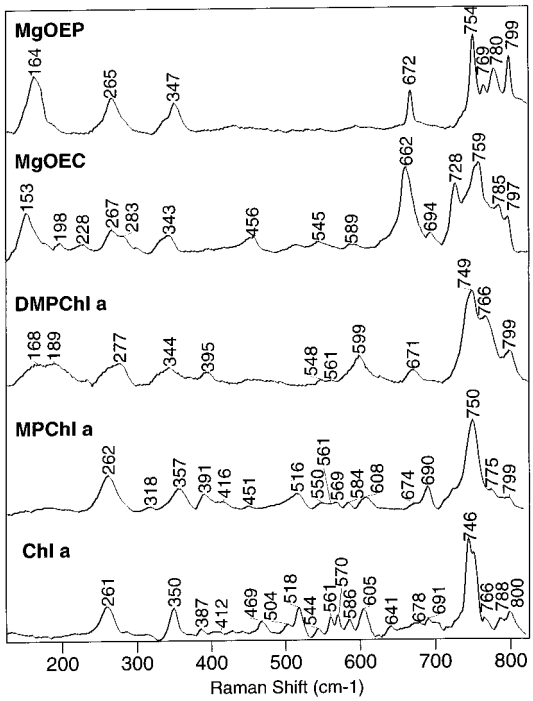

Figure 2. Low-frequency regions of the Q_y-excitation RR spectra of the films of the Mg(II) complexes obtained at 15 K. The exciting lines were as follows: MgOEP, $\lambda_{ex} = 580$ nm; MgOEC, DMPChl *a*, $\lambda_{ex} = 620$ nm; MPChl *a*, Chl *a*, $\lambda_{ex} = 647$ nm.

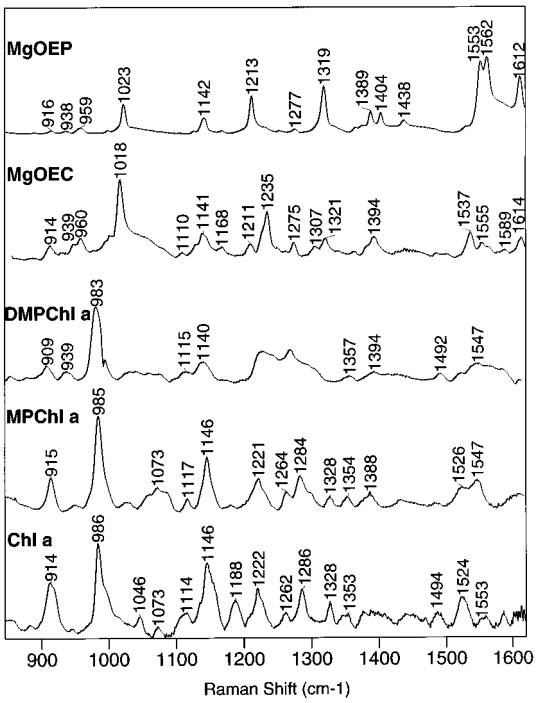

Figure 3. High-frequency regions of the Q_y-excitation RR spectra of films of the Mg(II) complexes obtained at 15 K. The exciting lines were as listed in the legend of Figure 2.

minimum energy structures, these groups generally assumed orientations that are substantially out of the pseudoplane of the macrocycle. Consequently, many of the low-frequency normal modes of the complexes and, in particular, those which contain substantial contributions from motions of the substituent groups cannot be classified as either in-plane or out-of-plane in character.

Results

Q_y-Excitation RR Spectra of Films. The low-frequency (100−825 cm^{-1}) regions of the low-temperature (15 K) Q_y-excitation RR spectra of films of MgOEP, MgOEC, DMPChl *a*, MPChl *a*, and Chl *a* are shown in Figure 2. The corresponding high-frequency (825−1600 cm^{-1}) spectra are shown in Figure 3. [For MgOEP, there is no distinction between the Q_y- and Q_x-states owing to (near) degeneracy in the higher symmetry complex (the electronic symmetry is retained, although the actual symmetry is lower).[24] However, for convenience, the designator Q_y-excitation will also be used to refer to the RR spectra of this complex.] The specific exciting lines used to obtain the spectra shown in both figures are given in the legend of Figure 2. All of the exciting lines fall on the high-energy side of the Q_y absorption band contour. The Q_y absorption maxima for all of the complexes in the film environment are shifted by 10 nm or less compared with solution.[17b] The RR spectra obtained with different exciting lines in the Q_y band contour are generally similar to those shown in the figures with respect to both number and frequency of the bands; however, some changes in relative intensity are observed among the various modes. The spectra obtained with excitation on the high-energy side of the Q_y absorption band contour are presented because excitation in this region generally yields the highest quality spectra.[17] In addition, the RR data acquisition window can be extended to larger wavenumber shifts before interference from fluorescence compromises the spectra.

Inspection of Figures 2 and 3 reveals that all of the complexes yield high-quality Q_y-excitation RR spectra. The fact that MgOEP and MgOEC yield good quality spectra demonstrates that the film technique is not specific to photosynthetic pigments in its utility for acquisition of Q_y-excitation RR data. Indeed, this method appears to be quite general inasmuch as Q_y-excitation RR spectra have been successfully obtained for every highly fluorescent complex examined to date in our laboratory (Ghosh, A.; Diers, J. R.; Bocian, D. F., unpublished results). Closer inspection of the figures reveals that the quality of the spectrum obtained for DMPChl *a* is somewhat poorer than that of the other complexes. This is particularly evident in the high-frequency region. The reason that DMChl *a* yields poorer quality spectra is uncertain, but most likely involves the detailed characteristics of the film that this complex forms. In the frequency regime above 1600 cm^{-1} (not shown), none of the complexes yield good quality spectra. This reduction in quality occurs because the RR wavenumber shift is sufficiently large that the spectral window falls into a region where there is considerable interference from fluorescence.

Inspection of Figures 2 and 3 reveals that all of the Mg(II) complexes exhibit rich RR spectra in both the low- and high-frequency regions. This behavior parallels that observed in the Q_y-excitation RR spectra of other photosynthetic pigments.[13,14,17] In general, the spectral complexity systematically increases as the structural complexities of Chl *a* are added to the basic tetrapyrrole architecture. In the low-frequency regime, most of the additional spectral features occur in the 350−750-cm^{-1} region. In the high-frequency regime, the additional features are spread throughout the entire spectral region. A particularly noteworthy observation is that very low-frequency (<250 cm^{-1}) RR bands which are prominent in the spectra of MgOEP and MgOEC are very weak or absent in the spectra of the structurally more complicated DMPChl *a*, MPChl *a*, and Chl *a* complexes.

Comparison of the RR spectra of the Mg(II) complexes with those previously reported for the Ni(II) analogues reveals that the spectra of the two different metalated complexes are very similar to one another.[18] Some differences are observed in the frequencies and relative intensities of certain RR bands. The frequency differences are expected because the Mg(II) and Ni-

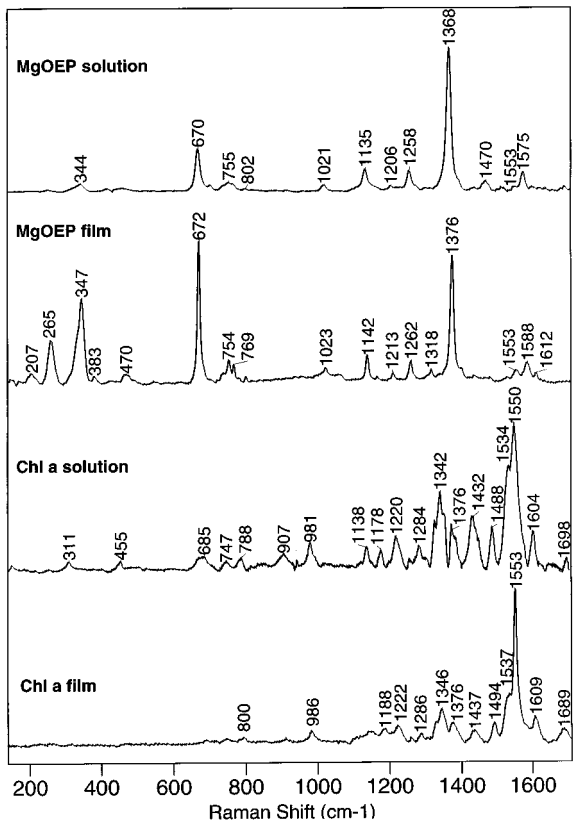

Figure 4. Comparison of the B-excitation ($\lambda_{ex} = 406.7$ nm) RR spectra of films (15 K) and solutions (293 K) of MgOEP and Chl *a*.

(II) have different ionic radii.[25] In addition, the Mg(II) ion is 5-coordinate, whereas the Ni(II) ion is 4-coordinate. The RR intensity differences occur primarily because the frequencies of the exciting lines versus the Q_y optical transitions are not identical in the experiments on the Mg(II) and Ni(II) complexes. The fact that the RR spectra of the Mg(II) and Ni(II) complexes are very similar lends credence to our earlier assignments of the high-frequency vibrational modes of Chl *a* (which were made exclusively via comparison with the Ni(II) complexes).[18]

B-Excitation RR Spectra of Films versus Solutions. One question that arises is whether the film environment significantly affects the RR spectral features observed for the Mg(II) complexes. To properly address this issue, it would be necessary to compare the Q_y-excitation RR spectra of film versus solution samples. Such studies are, of course, not feasible owing to the fluorescence emission from the solution samples. However, to gain some insight into the influence of the film environment, B-excitation RR spectra were obtained for both film and solution samples of selected complexes. Excitation in resonance with the higher energy B-state yields RR spectra free from fluorescence.[4a−c]

The B-excitation ($\lambda_{ex} = 406.7$ nm) RR spectra of Chl *a* in film and solution environments are compared in Figure 4 (bottom two traces). These data reveal that the RR frequencies and intensity-enhancement patterns are generally quite similar for the film versus solution samples. Most of the frequency differences are less than 5 cm^{-1}. One exception is the $\nu(C_9{=}O)$ stretching mode, which is observed at 1698 cm^{-1} (solution)[5] and 1689 cm^{-1} (film). The downshift of the $\nu(C_9{=}O)$ mode occurs because the oxygen atom of the $C_9{=}O$ group of a particular Chl *a* molecule in the film most likely serves as the axial ligand to the Mg(II) ion of an adjacent Chl *a* molecule.[17a]

The B-excitation ($\lambda_{ex} = 406.7$ nm) RR spectra of MgOEP in film and solution environments are also shown in Figure 4 (top two traces). The RR spectral signatures for MgOEP are more different in the film versus solution than those observed for Chl *a*. In particular, the RR intensity enhancements for the low-frequency ν_8 (347 cm^{-1}) and ν_9 (265 cm^{-1}) modes of MgOEP are quite large for the film sample but very weak for the solution sample. Both ν_8 and ν_9 involve vibrations of the relatively flexible β-ethyl substituents on the macrocycle.[26] Previous RR studies on different crystalline forms of NiOEP have shown that the RR intensity enhancements of these modes are very sensitive to the local environment.[26] The data reported herein for film samples corroborate this assessment. Despite the RR intensity differences observed for the low-frequency modes of MgOEP in the film versus solution environments, the frequencies of the modes are not significantly different.

Vibrational Assignments. The low-frequency modes (<1000 cm^{-1}) observed in the Q_y-excitation RR spectra of all the Mg(II) complexes are listed in Table 1 along with a proposed set of vibrational assignments. For reference, the normal mode assignments for NiOEP are also included in the table.[26] The normal mode descriptors listed in Table 1 are generic rather than specific in nature and indicate only the largest contributors to the vibrational eigenvectors. For DMPChl *a*, MPChl *a*, and Chl *a*, the presence of the isocyclic ring results in extremely complicated vibrational eigenvectors for virtually all of the modes (vide infra). These modes are characterized by contributions from a very large number of internal coordinates. Consequently, it is neither reasonable nor particularly informative to list the complete potential energy distribution in tabular format. Thus, the fact that certain modes of the different complexes are given the same generic normal mode descriptor is not meant to imply that the vibrational eigenvectors for these modes are in any sense identical. Likewise, the listing of the NiOEP mode assignments should not be construed to indicate that the vibrational eigenvectors of the saturated-pyrrole complexes are necessarily similar to those of this complex. Indeed, the correlations listed in the table are meant only to indicate that the modes of the different complexes have certain characteristics in common.

Discussion

The studies of the various Mg(II) tetrapyrrolic complexes reported herein demonstrate that the film technique permits the acquisition of Q_y-excitation RR spectra for a structurally diverse group of chromophores. The fact that the frequencies of the RR active modes of both the natural photosynthetic pigment Chl *a* and the porphyrin model complex MgOEP are similar in the film and solution environments lends credence to the argument that the film data are generally representative of the vibrational characteristics of the different type macrocycles. In the case of Chl *a*, the similarities between the film and solution spectra extend to the RR intensity enhancements, further suggesting that the film environment does not substantially alter the coupling between the vibrational modes and the electronic transition(s). In the sections below, we first discuss our strategy for assigning the RR spectra. We then examine the influence of the different structural elements on the low-frequency spectral features and normal mode characteristics. Finally, we comment on the implications of the present study for understanding vibronic interactions in natural photosynthetic systems.

Vibrational Assignment Strategy. The vibrational assignments for the low-frequency modes of the different Mg(II) complexes were determined in a stepwise and concerted fashion. The general procedure parallels that which we have previously used to assign the high-frequency modes of the Ni(II) analogues of these complexes.[18] The methodology is as follows.

(1) The RR spectra and calculated normal modes of MgOEP were compared with those of NiOEP.[26] This comparison

TABLE 1: Low-Frequency (<1000 cm^{-1}) Modes Observed with Q_y-Excitation[a]

MgOEP	MgOEC	DMPChl *a*	MPChl *a*	Chl *a*	assignment[b]	NiOEP assignment[c]
164	153	168			$\gamma C_\beta C_a$	γ_{17}
	198	189			δC_β alkyl	ν_{34}
	228				$\gamma\ C_\alpha C_m$	γ_{24}
265	267, 283	277	262	261	δC_β alkyl, $\gamma C_\beta C_a$	ν_9, γ_7
			318		δC_β alkyl	ν_{17}
347	343	344	357	350	$\delta C_\beta C_a$, $\gamma C_\beta C_a$	ν_8
		395	391	387	δring V, δring III	
			416	412	$\delta C_\beta C_c{=}C_d$	
	456		451		$\delta C_\beta C_1 C_2$	δ_4
				469	$\delta O_1 C_{carbo} O_2$, $\delta C_9{=}O$	
				504	$\delta O_1 C_{carbo} O_2$, $\delta C_9{=}O$	
			516	518	$\delta C_9{=}O$, δring III, δring V	
	545	548	550	544	$\gamma C_\beta C_a$, $\nu C_\beta C_a$	ν_{25}
		561	561	561	δring II, δring V, δring III	
			569	570	$\gamma(=C_dH_2)$as, γring I	
	589		584	586	$\delta C_\beta C_a H$, $\delta C_b C_a H$, $\delta C_\alpha C_m$	ν_{24}
		599	608	605	δring V, δring III	
				641	$\gamma O_1 C_{carbo} O_2$, γring V	
672	662	671	674	678	$\delta C_\alpha C_m C_\alpha$, $\nu C_\alpha N$, $\delta C_\alpha C_m$	ν_7
	694		690	691	δring IV	
	728				δpyr	ν_{16}
754	759	749	750	746	δpyr	ν_{15}
769, 780	785	766	775	766, 788	γCH_2 (rock)	γCH_2 (rock)
799	799	799	799	800	$\delta C_\alpha C_m C_\alpha$, $\nu C_\beta C_a$, νMgN	ν_6
916	914	909	915	914	$\delta C_\beta C_\beta$ alkyl, $\gamma(=C_dH_2)_s$	ν_{46a}
938	939	939			$\delta C_\beta C_\beta$ alkyl, $\delta C_b C_a H$	ν_{32}
959					δCH_3	δCH_3
		983	985	986	$\nu C_9 C_{10}$	

[a] MgOEP, $\lambda_{ex} = 580$ nm; MgOEC, DMPChl *a*, $\lambda_{ex} = 620$ nm; MPChl *a*, Chl *a*, $\lambda_{ex} = 647$ nm. [b] Mode descriptors are as follows: ν = stretch, δ = in-plane deformation, and γ = out-of-plane deformation. Symbols refer to the macrocycle and substituent positions shown in Figure 1. [c] NiOEP mode descriptions are those given in ref 26.

revealed that the spectral features are similar for the two complexes (vide infra). The vibrational frequencies and eigenvectors obtained for the metalloOEP complexes using the QCFF/PI method were also compared with those obtained via conventional valence force field methods.[26] This comparison revealed that the two computation methods yield generally similar results.

(2) The RR spectra and normal modes of MgOEC were compared with those of both MgOEP and NiOEP. This comparison included both the Q_y- and B-excitation data for the two porphyrins because the Q_y-excitation RR spectra of metallochlorins share features in common with both the B- and Q_y-excitation spectra of metalloporphyrins.[25c] In particular, B-excitation RR activity is derived from a Franck−Condon mechanism which gives rise to scattering from totally symmetric modes.[25a] In contrast, Q_y-excitation RR activity for metalloporphyrins is derived from a Herzberg−Teller mechanism which gives rise to scattering from non-totally symmetric modes.[25a] For MgOEC, and metallochlorins in general, Q_y-excitation RR activity is derived predominantly from a Franck−Condon mechanism; thus, totally symmetric modes are predominantly enhanced.[25b,c] Certain of these totally symmetric modes are derived from totally symmetric modes of metalloporphyrins (observed with B-excitation), whereas others are derived from non-totally symmetric (specifically b_{1g}) modes (observed with Q_y-excitation) which become symmetric in the lower symmetry environment.[25c] [In actuality, a number of totally symmetric modes gain significant RR activity in the Q_y-excitation spectra of MgOEP in films and NiOEP in certain crystalline forms.[26] For example, totally symmetric mode activity is particularly apparent in the low-frequency region, where ν_7 (672 cm^{-1}), ν_8 (347 cm^{-1}), and ν_9 (265 cm^{-1}) are very strongly enhanced.] The comparison of the Q_y-excitation RR spectra of MgOEC with the B- and Q_y-excitation spectra of both MgOEP and NiOEP permits the identification of qualitatively analogous features among the various complexes.

(3) After assigning the vibrational modes of MgOEC, the observed and calculated features of DMPChl *a*, MPChl *a*, and Chl *a* were examined and compared with one another and with those of MgOEC. For certain of the RR bands of the isocyclic ring containing complexes, the observed frequencies and intensity enhancement patterns allowed a relatively straightforward correlation with those of MgOEC. All of the low-frequency modes were then plotted in order to assess more critically the effects of the addition of the isocyclic ring and, ultimately, the $C_9{=}O$, C_2-vinyl, and C_{10}-carbomethoxy groups. In general, more modes are calculated than observed in the RR spectra. Many of these modes were removed from consideration because their eigenvectors did not contain contributions from internal coordinates in the new structural elements. However, in certain cases, multiple modes are calculated that both exhibit motions in the new structural element and fall very close in frequency to the observed RR band. In these cases, the mode closest in frequency to the observed mode was chosen for the assignment. Finally, we note that for a few vibrations classified as ring skeletal/β-alkyl modes, the calculated frequencies differ from the observed values by as much as 80 cm^{-1} (Table 1, vide infra). These disparities obviously reflect certain deficiencies in the QCFF/PI vibrational force field. Nevertheless, the fidelity between the observed and calculated frequencies is far better for the majority of the modes, lending confidence that the normal mode descriptors are qualitatively reasonable.

Influence of Different Structural Elements on the Low-Frequency Vibrational Characteristics. The influence of the different structural elements on the RR spectral features and normal mode characteristics is discussed below. First, we examine the ring-skeletal and alkyl-substituent vibrations. Next, we turn to the vibrational consequences of addition of the isocyclic ring. Finally, we describe the features associated with the $C_9{=}O$, C_2-vinyl, and C_{10}-carbomethoxy groups.

Ring-Skeletal and Alkyl-Substituent Modes. All of the Mg(II) complexes share the basic architecture of a tetrapyrrole

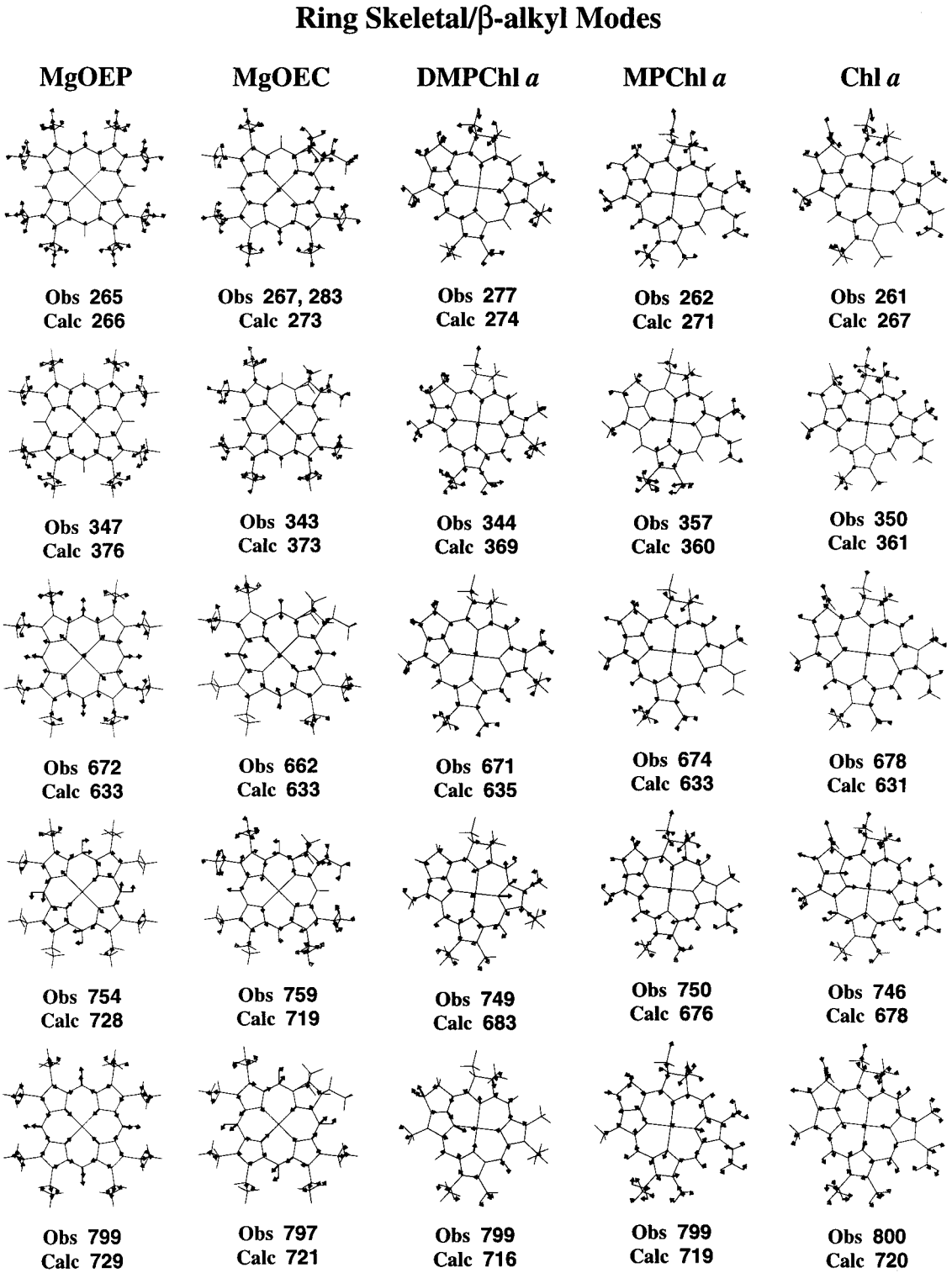

Figure 5. Vibrational eigenvectors of low-frequency ring-skeletal and β-alkyl substituent deformations which are common to all of the Mg(II) complexes. The arrows indicate motion in the $x-y$ pseudoplane of the macrocycle (see text).

containing alkyl substituents on each of the four pyrrole rings (Figure 1). Both MgOEP and MgOEC contain eight β-ethyl substituents, whereas DMPChl *a*, MPChl *a*, and Chl *a* contain methyl, ethyl, and propyl groups. The normal coordinate calculations predict that many of the low-frequency vibrational modes of the Mg(II) complexes primarily involve deformations of the inner-ring core of the tetrapyrrole or deformations of the substituent groups. Both types of vibrations are somewhat shielded from the effects of pyrrole ring saturation or addition of the isocyclic ring. Indeed, the low-frequency RR spectra of the various Mg(II) dihydroporphyrin complexes exhibit a number of features in common with one another and which are also observed in the spectra of MgOEP and/or NiOEP. In particular, bands are observed near 270, 350, 550, 670, 750, 770, 800, and 915 cm^{-1} for all of the complexes. For the Mg(II) dihydroporphyrins, these modes appear to be qualitative analogues of the porphyrinic vibrations classified as $\nu_9(\gamma_7)$, ν_8, ν_{25}, ν_7, ν_{15}, γCH_2 (rock), ν_6, and ν_{46a}, respectively.[26] [The 550 cm^{-1} (ν_{25}) band is observed for NiOEP in certain crystalline forms,[26] but not for the MgOEP film.] Other RR bands are observed for some but not all of the Mg(II) dihydroporphyrins, which fall at frequencies very similar to those observed for either

MgOEP and/or NiOEP. For example, MgOEC and DMPChl *a* exhibit bands near 160, 195, and 940 cm^{-1} which appear to be qualitative analogues of the γ_{17}, ν_{34}, and ν_{32} substituent deformations of metalloOEPs.[26] [Here again, the 195 cm^{-1} (ν_{34}) mode is observed for NiOEP in certain crystalline films,[26] but not for the MgOEP film.] Interestingly, these substituent deformations exhibit significant RR activity only in the Mg(II) dihydroporphyrins that contain multiple ethyl substituents. This RR activity could be induced either directly, as a result of ethyl group orientation, or indirectly, via ethyl-group-mediated structural changes in the macrocycle core that occur in the aggregate.

The computed vibrational eigenvectors for five ring-skeletal/β-alkyl substituent deformations that are observed in the RR spectra of all the Mg(II) complexes are plotted in Figure 5. In this figure and in all subsequent figures shown below, displacements are shown only for those atoms that contribute significantly to the normal mode (10% or greater of the maximum atomic displacement in a given mode). For all of these ring-skeletal/β-alkyl vibrations, the primary motions are in the $x-y$ pseudoplane of the molecule, consistent with their assignments as qualitative analogues of in-plane deformations of metalloporphyrins (vide supra). Inspection of the eigenvectors for the Mg(II) dihydroporphyrins, particularly those containing the isocyclic ring, reveals the complexity of the motions and, hence, the limited utility of attempting to describe the modes in a tabular format. This complexity is a general consequence of the effects of low symmetry on the vibrational characteristics of the deformation modes of tetrapyrrolic macrocycles.[18,25c,e] Accordingly, the pictorial format is the only reasonable mechanism for gaining insight into the characteristics of the normal modes.

Ring V Modes. The presence of an isocyclic ring is the common structural element that distinguishes all photosynthetic pigments from simple porphyrins or hydroporphyrins (Figure 1). As noted above, this structural element is in large part responsible for symmetry lowering and the accompanying increase in complexity of the normal modes. In addition, the presence of ring V introduces a number of new normal modes of vibration which can potentially gain enhancement in the RR spectrum. In particular, the RR spectra of DMPChl *a*, MPChl *a*, and Chl *a* all exhibit features near 390, 560, 600, and 985 cm^{-1} which are not observed in the spectra of MgOEP, NiOEP, or MgOEC. We attribute all of these bands to vibrations associated with ring V (Table 1). The 390, 560, and 600 cm^{-1} modes are deformations, whereas the 985 cm^{-1} is a stretching vibration associated with the single bonds in the ring.

The computed vibrational eigenvectors of four modes of DMPChl *a*, MPChl *a*, and Chl *a* which have no analogues in MgOEP or MgOEC and whose frequencies are consistent with those observed for the ring V vibrations are plotted in Figure 6. For all of these vibrations, the primary motions are in the $x-y$ pseudoplane of the molecule. Inspection of Figure 6 reveals that the eigenvectors for all of the modes are complex and involve motions of many atoms in addition to those explicitly associated with ring V. Consequently, the designator "ring V vibration" is only a generic descriptor that indicates the occurrence of a normal mode that does not occur in architectures that lack this structural element.

C_9=O Modes. All photosynthetic pigments contain a keto group at the C_9-position of ring V (Figure 1). This group conjugates into the π-electron system of the macrocycle. The addition of the C_9=O group to the DMPChl *a* skeleton introduces only two new normal modes of vibration which could occur in the low-frequency regime, namely the in-plane and out-of-plane deformations of the C_9=O group. Both of these

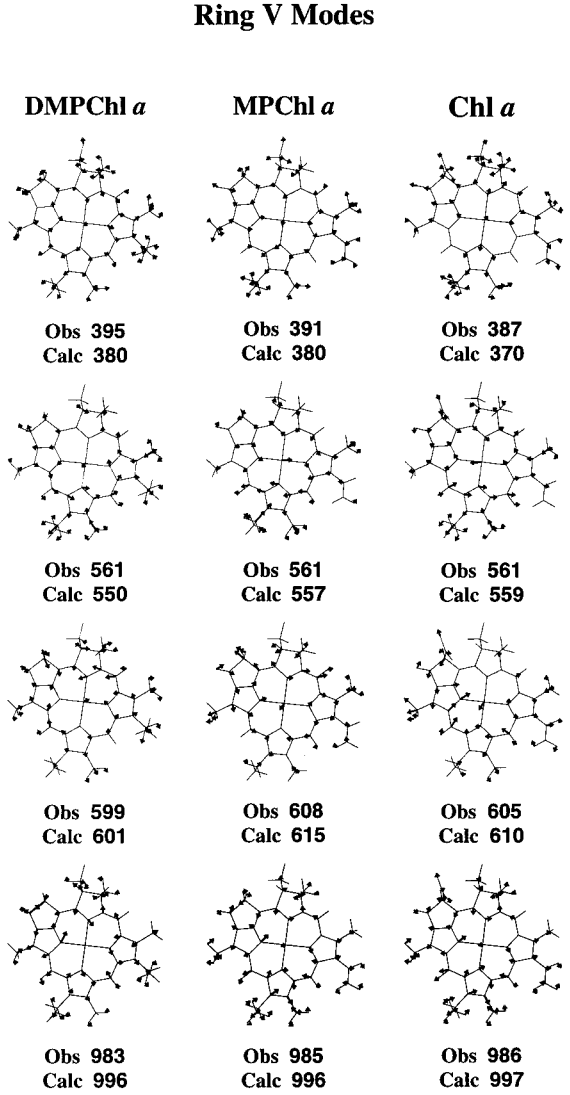

Figure 6. Vibrational eigenvectors of low-frequency modes that contain subtantial contributions from or occur due to the presence of, ring V. The arrows indicate motion in the $x-y$ pseudoplane of the macrocycle (see text).

vibrations are observed in the 400−500-cm^{-1} region in five-member-ring molecules such as cyclopentanone.[27] Comparison of the RR spectra of MPChl *a* and Chl *a* with those of DMPChl *a* reveals that the addition of the C_9=O group results in the appearance of only one additional RR band in the 400−500 cm^{-1} region. This band is observed near 517 cm^{-1} for both complexes. This spectral characteristic of the Mg(II) complexes is similar to that previously reported for the Ni(II) analogues, both of which exhibit a single new band near 534 cm^{-1}.[18] We attribute these features in both the Mg(II) and Ni(II) complexes to one of the two deformations of the C_9=O group.

The computed vibrational eigenvectors for modes unique to MPChl *a* and Chl *a* and whose composition and frequency are commensurate with a C_9=O deformation are plotted in Figure 7. The majority of the C_9=O motion is in the $x-y$ pseudoplane of the molecule; hence, the mode is classified as the in-plane deformation, δC_9=O. [The out-of-plane deformation, γC_9=O, is predicted near 400 cm^{-1}.] However, as is the case for the other modes associated with ring V, the eigenvector of the δC_9=O vibration contains substantial motions for other atoms in the macrocycle, particularly in the ring III−V region.

C_2-Vinyl Modes. Both MPChl *a* and Chl *a* contain a vinyl group at the C_2-position on pyrrole ring I (Figure 1). The RR scattering characteristics of vinyl substituents on porphyrins have

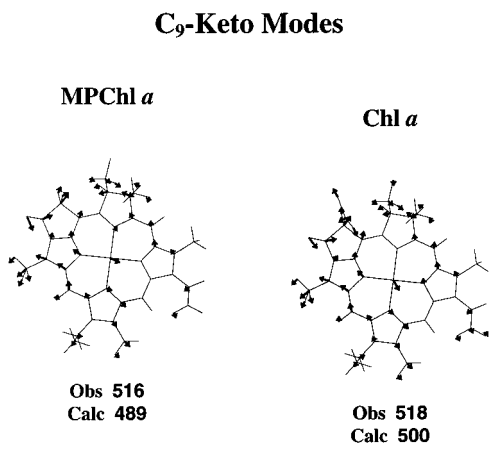

Figure 7. Vibrational eigenvectors of low-frequency modes that contain subtantial contributions from the C_9═O group. The arrows indicate motion in the $x-y$ pseudoplane of the macrocycle (see text).

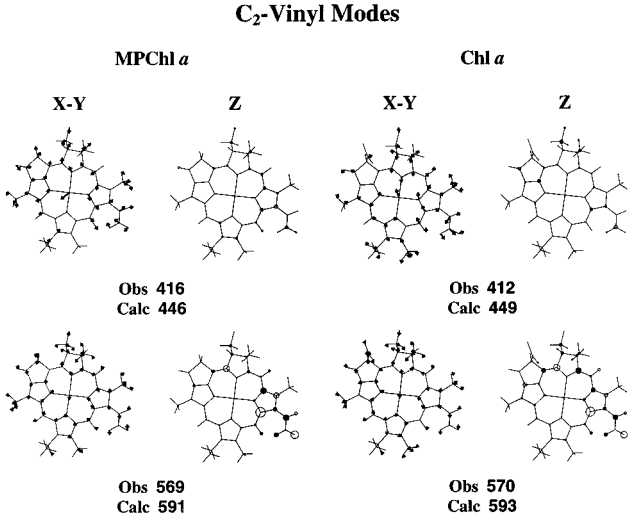

Figure 8. Vibrational eigenvectors of low-frequency modes that contain subtantial contributions from the C_2-vinyl group. Motions in both the $x-y$ pseudoplane of the macrocycle (arrows) and along the z-axis (circles) are shown (see text).

been extensively investigated because these groups are present on the protoheme IX prosthetic group of myoglobin, hemoglobin, and the *b*-type cytochromes.[28−34] In the low-frequency region, there are three normal modes of the C_2-vinyl group that could contribute to the RR spectrum, in particular, the deformation of the entire vinyl group, $\delta C_\beta C_c{=}C_d$, and the antisymmetric and symmetric out-of-plane deformations of the terminal vinyl hydrogens, $\gamma(=C_dH_2)_{as}$ and $\gamma(=C_dH_2)_a$. The $\delta C_\beta C_c{=}C_d$ and $\gamma(=C_dH_2)_s$ modes are observed in the RR spectra of protoheme IX near 400 and 920 cm^{-1}, respectively.[31,34] The $\gamma(=C_dH_2)_{as}$ mode has not been observed but is expected near 630 cm^{-1}.[34] The RR spectra of both MPChl *a* and Chl *a* exhibit bands near 412 and 570 cm^{-1} which are not observed for DMPChl *a*, MgOEC, or MgOEP. We attribute these RR bands to $\delta C_\beta C_c{=}C_d$ and $\gamma(=C_dH_2)_{as}$, respectively. The frequency of the $\gamma(=C_dH_2)_{as}$ mode is somewhat lower than has been previously suggested.[34] However, the normal coordinate calculations reported herein in fact predict a lower frequency for this mode in the photosynthetic pigments (vide infra). Both MPChl *a* and Chl *a* also exhibit a band near 920 cm^{-1} which could be due to $\gamma(=C_dH_2)_s$. However, all of the other Mg(II) complexes also exhibit a RR band near 920 cm^{-1} (Figure 2). Accordingly, we have assigned this band as a $\delta C_\beta C_\beta$alkyl mode (Table 1). Nevertheless, the 920 cm^{-1} RR bands of both MPChl *a* and Chl *a* are considerably stronger than the analogous bands of the other three complexes. This observation could indicate that bands due to both the $\gamma(=C_dH_2)_s$ and $\delta C_\beta C_\beta$alkyl are present and coincident. This issue can only be resolved via selective isotopic labeling of the C_2-vinyl group.

The computed vibrational eigenvectors for modes unique to MPChl *a* and Chl *a* and whose composition and frequency are commensurate with the $\delta C_\beta C_c{=}C_d$ and $\gamma(=C_dH_2)_{as}$ deformations are plotted in Figure 8. The majority of the atomic motion for the former mode is in the $x-y$ pseudoplane of the molecule, whereas the majority of the motion for the latter is along the z-axis. However, both modes exhibit displacements along the other coordinates because the C_2-vinyl group is not in the pseudoplane of the macrocycle. In addition, the eigenvectors for both the $\delta C_\beta C_c{=}C_d$ and $\gamma(=C_dH_2)_{as}$ deformations contain substantial contributions from motions in other parts of the molecule. This characteristic of the motion may explain why the $\gamma(=C_dH_2)_{as}$ vibration is RR active in the photosynthetic pigments but not in protoheme IX and also why its frequency is lower than anticipated (570 vs 630 cm^{-1}).

C_{10}-Carbomethoxy Modes. Chl *a* contains a carbomethoxy group at the C_{10} position on ring V (Figure 1). This structural element distinguishes the natural pigment from MPChl *a* (the propionate esters are also different in the two pigments; however, this does not influence the RR spectrum[18]). Previous high-frequency RR studies of (bacterio)chlorophylls have shown that the stretching vibration, $\nu C_{carbo}{=}O_1$, is resonance enhanced despite the fact that it is not conjugated into the π-system of the macrocycle.[6a,c,35] This raises the possibility that other vibrations of the C_{10}-carbomethoxy group could gain RR activity. In the low-frequency regime such modes would be deformations of the entire group with respect to ring V or deformations of the $O_1C_{carbo}O_2$ element. Inspection of the RR spectra of Chl *a* reveals that bands are observed near 469, 504, and 641 cm^{-1} which are not observed in the spectra of MPChl *a*. We attribute these modes to deformations involving the C_{10}-carbomethoxy group.

The computed vibrational eigenvectors for modes unique to Chl *a* and whose composition and frequency are commensurate with C_{10}-carbomethoxy group deformations are plotted in Figure 9. The eigenvectors for all three of these vibrations exhibit displacement in all three dimensions owing to the direction of the bond vector connecting the C_{10}-carbomethoxy group to ring V and the torsional angle of the group. As is the case for the deformations of other substituent groups, the eigenvectors for deformations of the C_{10}-carbomethoxy group contain substantial contributions from motions in other parts of the molecule. This coupling most likely explains the RR activity for these modes.

Implications for Photosynthetic Assemblies. The special pair primary electron donor of bacterial photosynthetic reaction center proteins ((BChl *a*)$_2$) and the BChl *c*/*d*/*e* aggregates of chlorosomal light-harvesting assemblies of green photosynthetic bacteria share the common feature that a number of very low-frequency vibrations (<250 cm^{-1}) are very strongly coupled to their photophysically important, lowest energy electronic transitions (which involve the Q_y-excited states of the pigments).[7−15c,16] The magnitude of the vibronic coupling for these modes is much larger than that for the other low- (and high-) frequency modes that are coupled to the Q_y-transition. The studies reported herein for Chl *a* and those reported previously for bacteriochlorophyll (BChl) *a*, both in film aggregates[17a] and in reaction center proteins,[13c−e] indicate that the low-frequency vibrational modes that are coupled to the Q_y-transition are diverse in character, ranging from vibrations of the tetrapyrrole skeleton to deformations of the peripheral substituent groups. However, the majority of the vibronically coupled modes in the lowest

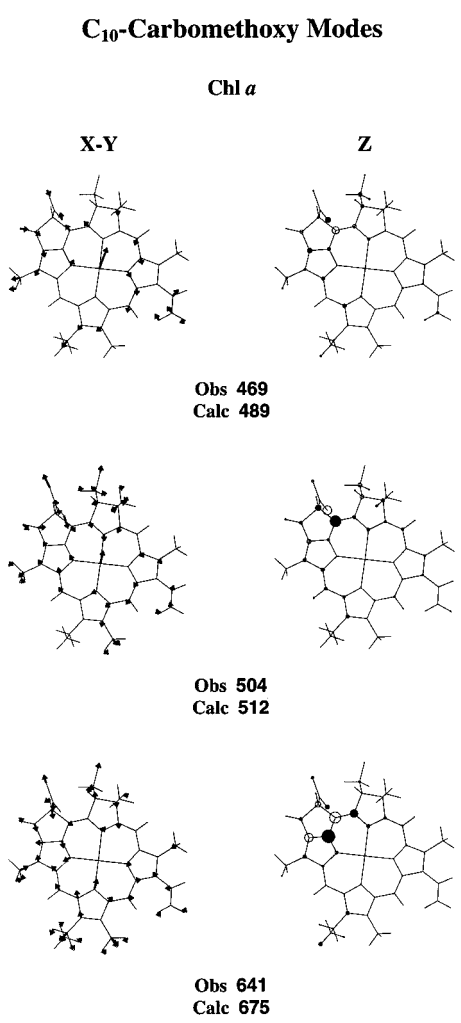

Figure 9. Vibrational eigenvectors of low-frequency modes that contain subtantial contributions from the C_{10}-carbomethoxy group. Motions in both the $x-y$ pseudoplane of the macrocycle (arrows) and along the z-axis (circles) are shown (see text).

frequency regime (<250 cm^{-1}) are due to deformations of the peripheral substituent groups.

Recently, our group has proposed a complete set of vibrational assignments for the very low-frequency modes of the $BChl_2$ and monomeric BChl *a* cofactors in bacterial reaction center proteins.[13d,e] These assignments indicate that the vibrations that exhibit greatly enhanced vibronic coupling in $BChl_2$ primarily involve motions of peripheral substituent groups appended to ring I of each of the BChl *a* molecules in the dimer. The structure of $BChl_2$ is such that the region of direct electronic overlap involves ring I of the two BChl *a* molecules.[36] Presumably, the deformations of the substituents on ring I become strongly coupled to the electronic transition because they effectively modulate the electronic overlap in the supermolecular structure.[13c,d]

In the case of the BChl *c*/*d*/*e* aggregates of chlorosomal light-harvesting assemblies, the nature of the very low-frequency modes which are strongly coupled to the lowest energy electronic transition(s) has not yet been elucidated. However, previous exploratory studies from our laboratory have revealed that these modes are most likely vibrations intrinsic to the BChl *c*/*d*/*e* chromophore[17b] (as is the case for the very strongly coupled modes of $(Bchl)_2$[13c,d]) rather than being new vibrations associated with the supermolecular assembly. The studies reported herein provide additional insight into the probable nature of the very strongly coupled low-frequency vibrations of Bchl *c*/*d*/*e* pigments. In particular, BChl *c*/*d*/*e* pigments are structurally similar to Chl *a* in that they are chlorins/dihydroporphyrins (one saturated pyrrole ring) rather than bacteriochlorins/tetrahydroporphyrins (two saturated pyrrole rings).[37] The key structural element that distinguishes BChl *c*/*d*/*e* from Chl *a* is that the C_2-vinyl group of the latter pigment is hydrated in the former, yielding an alcohol, $C_cH(OH)C_dH_3$. The hydoxyl group of the alcohol mediates the strong association of BChl *c*/*d*/*e* which occurs both in chlorosomes and for free pigments in solution.[37] The vibrational characteristics exhibited by Chl *a* and the other Mg(II) complexes studied herein suggest that most of the modes below 250 cm^{-1} involve deformations of the peripheral substituent groups. Accordingly, the very strongly coupled very low-frequency modes of BChl *c*/*d*/*e* most likely also involve motions of these groups. Deformations of the unique $C_cH(OH)$-C_dH_3 group of the Bchl *c*/*d*/*e* pigments are the best candidates for these vibrations. Deformations of this group could modulate the interchromophore separation between and, hence, the magnitude of the electronic coupling. The fact that deformations of the substituent groups are invariably mixed with motions involving the π-electron framework provides an additional mechanism for modulating the electronic structure of the aggregate. Together, the properties of $BChl_2$ and the BChl *c*/*d*/*e* aggregates suggest that modulation of electronic interactions via peripheral substituent groups is a general motif for controlling electronic communication in photosynthetic assemblies.

Acknowledgment. We thank Professor K. M. Smith for helpful suggestions concerning the preparation of DMPChl *a*. This work was supported by Grant GM36243 (D.F.B.) from the National Institute of General Medical Sciences.

References and Notes

(1) For recent treatises, see: (a) *Chlorophylls*; Scheer, H., Ed.; CRC Press: Boca Raton, FL, 1991. (b) *The Photosynthetic Reaction Center*; Deisenhofer, J., Norris, J. R., Eds.; Academic: San Diego, CA, 1993; Vols. I and II. (c) *Anoxygenic Photosynthetic Bacteria*; Blankenship, R. E., Madigan, M. T., Bauer, C. E., Eds.; Kluwer Acdemic Publishers: Dordrect, 1995.

(2) (a) Reference 1a, sections 4 and 5. (b) Barkigia, K. M.; Fajer, J. In ref 1b; Vol. II, pp 513- 540. (c) Reference 1c, sections IV and V.

(3) Myers, A. B.; Mathies, R. A. In *Biological Applications of Raman Spectroscopy*; Spiro, T. G., Ed.; Wily: New York, 1987; Vol. 2, pp 1−58.

(4) For reviews see (a) Lutz, M. *Adv. Infrared Raman Spectrosc.* **1984**, *11*, 211. (b) Lutz, M.; Robert, B. In *Biological Applications of Raman Spectroscopy*; Spiro, T. G., Ed.; Wiley: New York, 1988; Vol. 3, pp 347−411. (c) Lutz, M.; Mäntele, W. In ref 1a; pp 855−902. (d) Lutz, M. *Biospectroscopy* **1995**, *1*, 313.

(5) (a) Robert, B.; Lutz, M. *Biochemistry* **1988**, *27*, 5108. (b) Mattioli, T. A.; Hoffman, A.; Robert, B.; Schrader, B.; Lutz, M. *Biochemistry* **1991**, *30*, 4648. (c) Mattioli, T. A.; Hoffman, A.; Sockalingum, D. G.; Robert, B.; Lutz, M. *Spectrochim. Acta* **1993**, *49A*, 785. (d) Feiler, U.; Albouy, D.; Mattioli, T. A.; Lutz, M.; Robert, B. *Biochemistry* **1994**, *33*, 7594. (e) Mattioli, T. A. *J. Mol. Struct.* **1995**, *347*, 459.

(6) (a) Bocian, D. F.; Boldt, N. J.; Chadwick, B. A.; Frank, H. A. *FEBS Lett.* **1987**, *214*, 92. (b) Peloquin, J. M.; Violette, C. A.; Frank, H. A.; Bocian, D. F. *Biochemistry* **1990**, *29*, 4892. (c) Palaniappan, V.; Martin, P. C.; Chynwat, V.; Frank, H. A.; Bocian, D. F. *J. Am. Chem. Soc.* **1993**, *115*, 12035.

(7) (a) Meech, S. R.; Hoff, A. J.; Wiersma, D. A. *Chem. Phys. Lett.* **1985**, *121*, 287. (b) Meech, S. R.; Hoff, A. J.; Wiersma, D. A. *Proc. Natl. Acad. Sci. U.S.A.* **1986**, *83*, 9464.

(8) (a) Boxer, S. G.; Lockhart, D. J.; Middendorf, T. R. *Chem. Phys. Lett.* **1986**, *123*, 476. (b) Middendorf, T. R.; Mazzola, L. T.; Gaul, D. F.; Schenck, C. C.; Boxer, S. G. *J. Phys. Chem.* **1991**, *95*, 10142.

(9) (a) Hayes, J. M.; Small, G. J. *J. Phys. Chem.* **1986**, *90*, 4928. (b) Johnson, S. G.; Tang, D.; Jankowiak, R.; Hayes, J. M.; Small, G. J.; Tiede, D. M. *J. Phys. Chem.* **1989**, *93*, 5953. (c) Johnson, S. G.; Tang, D.; Jankowiak, R.; Hayes, J. M.; Small, G. J.; Tiede, D. M. *J. Phys. Chem.* **1990**, *94*, 5849. (d) Lyle, P. A.; Kolaczkowski, S. V.; Small, G. J. *J. Phys. Chem.* **1993**, *97*, 6924. (e) Hayes, J. M.; Lyle, P. A.; Small, G. J. *J. Phys. Chem.* **1994**, *98*, 7337.

(10) Klevanik, A. V.; Ganago, A. O.; Shkuropatov, A. Y.; Shuvalov, V. A. *FEBS Lett.* **1988**, *237*, 61.

(11) (a) Vos, M. H.; Lambry, J.-C.; Robles, S. J.; Youvan, D. C.; Breton, J.; Martin, J.-L. *Proc. Natl. Acad. Sci. U.S.A.* **1991**, *88*, 8885. (b) Vos, M.

H.; Lambry, J.-C.; Robles, J.; Youvan, D. C.; Breton, J.; Martin, J.-L. *Proc. Natl. Acad. Sci. U.S.A.* **1992**, *898*, 613. (c) Vos, M. H.; Rappport, F.; Lambry, J.-C.; Breton, J.; Martin, J.-L. *Nature* **1993**, *363*, 320. (d) Vos, M. H.; Jones, M. R.; Hunter, C. N.; Breton, J.; Lambry, J.-C.; Martin, J.-L. *Biochemistry* **1994**, *33*, 6750. (e) Vos, M. H.; Jones, M. R.; McGlynn, P.; Hunter, C. N.; Breton, J.; Martin, J.-L. *Biochim. Biophys. Acta* **1994**, *1186*, 117. (f) Vos, M. H.; Jones, M. R.; Hunter, C. N.; Breton, J.; Lambry, J.-C.; Martin, J.-L. *Proc. Natl. Acad. Sci. U.S.A.* **1994**, *91*, 12701.

(12) Stanley, R. J.; Boxer, S. G. *J. Phys. Chem.* **1995**, *99*, 859.

(13) (a) Donohoe, R. J.; Dyer, R. B.; Swanson, B. I.; Violette, C. A.; Frank, H. A.; Bocian, D. F. *J. Am. Chem. Soc.* **1990**, *112*, 6716. (b) Palaniappan, V.; Aldema, M. A.; Frank, H. A.; Bocian, D. F. *Biochemistry* **1992**, *31*, 11050. (c) Palaniappan, V.; Schenck, C. C.; Bocian, D. F. *J. Phys. Chem.* **1995**, *99*, 17049. (d) Czarnecki, K.; Diers, R. J.; Chynwat, V.; Erickson, J. P.; Frank, H. A.; Bocian, D. F. *J. Am. Chem. Soc.* **1997**, *119*, 415. (e) Czarnecki, K.; Chynwat, V.; Erickson, J. P.; Frank, H. A.; Bocian, D. F. *J. Am. Chem. Soc.* **1997**, *119*, 2594.

(14) (a) Shreve, A. P.; Cherepy, N. J.; Franzen, S.; Boxer, S. G.; Mathies, R. A. *Proc. Natl. Acad. Sci. U.S.A.* **1991**, *88*, 11207. (b) Cherepy, N. J.; Shreve, A. P.; Moore, L. J.; Franzen, S.; Boxer, S. G.; Mathies, R. A. *J. Phys. Chem.* **1994**, *98*, 6023. (c) Cherepy, N. J.; Holzwarth, A.; Mathies, R. A. *Biochemistry* **1995**, *34*, 5288.

(15) (a) Savikhin, S.; Zhu, Y.; Lin, S.; Blankenship, R. E.; Struve, W. S. *J. Phys. Chem.* **1994**, *98*, 10322. (b) Savikin, S.; van Noort, P. I.; Zhu, Y.; Lin, S.; Struve, W. S. *Chem. Phys.* **1995**, *194*, 245. (c) Savikin, S.; van Noort, P. I.; Blankenship, R. E.; Struve, W. S. *Biophys. J.* **1995**, *69*, 1100. (d) Savikhin, S.; Struve, W. S. *Photosynth. Res.* **1996**, 48, 271. (e) Chachivilis, M.; Pulerits, T.; Jones, M. R.; Hunter, C. N.; Sundström, V. In *Ultrafast Phenomena IX*; Barbara, P., Knox, W. H., Mourou, G. A., Zewail, A. H., Eds.; Sringer: Berlin, 1994; pp 435−436.

(16) Cherepy, N. J.; Du, M.; Holzwarth, A. R.; Mathies, R. A. *J. Phys. Chem.* **1996**, *100*, 4662.

(17) (a) Diers, J. R.; Bocian, D. F. *J. Am. Chem. Soc.* **1995**, *117*, 6629. (b) Diers, J. R.; Zhu, Y.; Blankenship, R. E.; Bocian, D. F. *J. Phys. Chem.* **1996**, *100*, 8573.

(18) Boldt, N. J.; Donohoe, R. J.; Birge, R. R.; Bocian, D. F. *J. Am. Chem. Soc.* **1987**, *109*, 9, 2284.

(19) (a) Warshel, A.; Karplus, M. *J. Am. Chem. Soc.* **1972**, *94*, 5612. (b) Warshel, A.; Levitt, M. *Quantum Chemistry Program Exchange*, No. 247, Indiana Unisverisy, 1974.

(20) Lindsey, J. S.; Woolford, J. N. *Inorg. Chem.* **1995**, *34*, 1063.

(21) Whitlock, H. W., Jr.; Hanauer, R.; Oester, M. Y.; Bower, D. K. *J. Am. Chem. Soc.* **1969**, *91*, 7485.

(22) Smith, K. M.; Goff, D. A.; Simpson, D. J. *J. Am. Chem. Soc.* **1985**, *107*, 4946.

(23) Abraham, R. J.; Rowan, A. E.; Smith, N. W.; Smith, K. M. *J. Chem. Soc., Perkin Trans.* **1993**, *2*, 1047.

(24) Gouterman, M. In *The Porphyrins*; Dolphin, D., Ed.; Academic: New York, 1978; Vol. 3, pp 1−165.

(25) (a) Spiro, T. G. In *Iron Porphyrins*; Lever, A. B. P., Gray, H. B., Eds.; Addison Wesley: Reading, MA, 1983; Vol. 2, pp 89−160. (b) Kitagawa, T.; Ozaki, Y. *Struct. Bonding* **1987**, *64*, 71. (c) Schick, G. A.; Bocian, D. F. *Biochim. Biophys. Acta* **1987**, *895*, 127. (d) Spiro, T. G.; Czernuszewicz, R. S.; Li, X.-Y. *Coord. Chem. Rev.* **1990**, *100*, 541. (e) Procyk, A. D.; Bocian, D. F. *Annu. Rev. Phys. Chem.* **1992**, *43*, 456.

(26) (a) Li, X.-Y.; Czernuszewicz, R. S.; Kincaid, J. R.; Spiro, T. G. *J. Am. Chem. Soc.* **1989**, *111*, 7012. (b) Li, L.-Y.; Czernuszewicz, R. S.; Kincaid, J. R.; Stein, P.; Spiro, T. G. *J. Phys. Chem.* **1990**, *94*, 47.

(27) Kartha, V. B.; Mantsch, H. H.; Jones, R. N. *Can. J. Chem.* **1973**, *51*, 1749.

(28) (a) Choi, S.; Spiro, T. G.; Langry, K. C.; Smith, K. M.; Budd, D. L.; LaMar, G. N. *J. Am. Chem. Soc.* **1982**, *104*, 4337. (b) Choi, S.; Spiro, T. G.; Langry, K. C.; Smith, K. M.; Budd, D. L.; LaMar, G. N. *J. Am. Chem. Soc.* **1982**, *104*, 4345.

(29) Lee, H.; Kitagawa, T.; Abe, M.; Pandey, R. K.; Smith, K. M. *J. Mol. Struct.* **1986**, *146*, 329.

(30) Sage, J. T.; Morikis, D.; Champion, P. M. *J. Chem. Phys.* **1989**, *90*, 3015.

(31) Gersonde, K.; Yu, N.-T.; Lin, S. H.; Smith, K. M.; Parish, D. W. *Biochemistry* **1989**, *28*, 8197.

(32) DeVito, V. L.; Cai, M. Z.; Asher, S. A.; Kehres, L. A.; Smith, K. M. *J. Phys. Chem.* **1992**, *96*, 6917.

(33) Kalsbeck, W. A.; Ghosh, A.; Pandey, R. K.; Smith, K. M.; Bocian, D. F. *J. Am. Chem. Soc.* **1995**, *117*, 10959.

(34) Hu, S.; Smith, K. M.; Spiro, T. G. *J. Am. Chem. Soc.* **1996**, *118*, 12638.

(35) (a) Heald, R. L.; Callahan, P. M.; Cotton, T. M. *J. Phys. Chem.* **1988**, *92*, 4820. (b) Heald, R. L.; Cotton, T. M. *J. Phys. Chem.* **1990**, *94*, 3968.

(36) For an overview of reaction center structure, see: Ermler, U.; Fritzsch, G.; Buchanan, S.; Michel, H. *Structure* **1994**, *2*, 925.

(37) Blankenship, R. E.; Olson, J. M.; Miller, M. In ref 1c, pp 399−435.